# Strain engineered ferromagnetism in $LaMnO_3$ thin films

*Jaume Roqueta[1], Alberto Pomar[2], Lluis Balcells[2], Carlos Frontera[2], Sergi Valencia[4], Radu Abrudan[4,5], Bernat Bozzo[2], Zorica Konstantinovic[2,3], José Santiso[1] and Benjamín Martínez[2]*

[1]Institut Català de Nanociència i Nanotecnologia, ICN2 (CSIC-ICN), Campus de la UAB, 08193,Bellaterra, SPAIN

[2]Instituto de Ciencia de Materiales de Barcelona – CSIC, Campus de la UAB, 08193 Bellaterra, SPAIN

[3] Center for Solid State Physics and New Materials, Institute of Physics Belgrade, University of Belgrade, Pregrevica 118, 11080 Belgrade, SERBIA

[4]Helmholtz-Zentrum-Berlin für Materialien und Energie, Albert-Einstein Str. 15, D-12489 Berlin, GERMANY

[5]Institut für Experimentalphysik/Festkörperphysik, Ruhr-Universität Bochum, 44780 Bochum, GERMANY

KEYWORDS: Oxide thin films, Strain induced effects, Magnetism

ABSTRACT. A systematic study of the growth process of $LaMnO_3$ (LMO) thin films, by pulsed laser deposition, on top of $SrTiO_3$ substrates under different oxygen partial pressures ($PO_2$) is reported. It is found that the accommodation of the orthorhombic LMO phase onto the cubic STO structure, i.e. the amount of structural strain, is controlled by background oxygen pressure. We demonstrate that magnetic behaviour can be continuously tuned from robust ferromagnetic (FM) ordering to an antiferromagnet. These results strongly point to a strain-induced selective orbital occupancy as the origin of the observed FM behaviour, in agreement with recent theoretical calculations.

## INTRODUCTION

The $LaMnO_3$ (LMO) perovskite compound has gained renewed interest for being an essential building block in some heterostructures showing emerging phenomena as, for instance, unexpected exchange bias in $LaMnO_3/LaNiO_3$ multilayers[1] or the evidence of ferromagnetism (FM) at the interface of $LaMnO_3/SrTiO_3$ [2-3] or $LaMnO_3/SrMnO_3$ [4] heterostructures. Irrespective to the growth conditions used in those works, LMO layers were reported to exhibit robust FM behaviour in contrast to the antiferromagnetic (AF) character of the ground state of the stoichiometric LMO bulk material, where $Mn^{3+}$ magnetic moments are arranged in an A-type AF ordering.[5-7] This unexpected FM character has been often detected in LMO films and in spite of several attempts to explain it, its origin is still unclear. First, it is known that LMO perovskite structure cannot accommodate oxygen excess at interstitial positions and thus, it must be accommodated by the creation of La and/or Mn vacancies. [5] In this scenario, to compensate the charge unbalance, a $Mn^{3+/4+}$ mixed valence state is invoked and therefore, the observed ferromagnetism is simply explained by a double exchange mechanism with the concomitant tendency to metallic behaviour, similar to doped manganites. [8-10] However, this explanation is in contradiction with some experimental results evidencing a FM-insulating (I) behaviour that should be excluded in a canonical double exchange model.[11-14] To solve this puzzling situation several extrinsic origins have been proposed to account for the observed FM behaviour. Most of them are based on a non-stoichiometric La:Mn relationship[8, 12, 14] and a multiple double exchange mechanism by the creation of $Mn^{2+}$ ions.[15-16] On the other hand, strain effects due to the film/substrate mismatching have also been invoked in some cases. As shown by theoretical studies, strain may lead to different patterns of octahedral distortions, either by Jahn-Teller distortions or by oxygen octahedral rotations, thus promoting selective magnetic/orbital

arrangements.[17-21] Therefore, since magnetic and orbital ordering in LMO are directly corelated to the particular arrangement and configuration of the $MnO_6$ octahedral framework, it is clear that strain may strongly affect its magnetotransport properties.[6, 22] This possibility has raised new interest since strain-induced FM has already been reported in other manganese thin films. Quite recent first-principle calculations suggest that, in fact, FM-I could be an intrinsic ground state in these manganese oxides under some given values of biaxial strain.[23] In this scenario, the change in the magnetic order (AF/FM) would be explained as due to the occurrence of a novel $d_{3z^2-r^2}/d_{x^2-y^2}$ alternated orbital ordering that is stabilized in the distorted $MnO_6$ octahedra of the strained LMO monoclinic cell.

In this work we report on the magnetic, transport and structural properties of LMO thin films grown on $SrTiO_3$ (STO) substrates. The influence of oxygen partial pressure ($PO_2$) during the growth process on the accommodation of the orthorhombic LMO phase onto the cubic STO structure is thoroughly analyzed. Our results demonstrate that magnetic behaviour can be continuously tuned from a robust FM to an AF depending on the amount of structural strain accumulated in the structure. Our findings will be analysed in terms of recent theoretical calculations suggesting different orbital orderings in LMO as a function of biaxial strain.

## EXPERIMENTAL DETAILS

$LaMnO_3$ thin films have been grown on top of (100)STO single crystalline substrates by Pulsed Laser Deposition (PLD) at substrate temperatures between 700 °C and 900 °C and under a wide range of background oxygen partial pressures (from 200 mTorr down to $5x10^{-3}$ mTorr). Laser fluence was kept constant at 0.8 J/cm$^2$. The number of pulses was adjusted to obtain film thicknesses in the range of 35-45 nm. The thickness of the films was determined by x-ray reflectometry and by contact profilometry. Systematic x-ray diffraction characterization was

carried out in a four-angle diffractometer with a Cu-$K_\alpha$ radiation source (X´Pert MRD-Panalytical) and a Bruker D8 Advance GADDS system. Phase purity and structural quality of the films was confirmed by standard θ-2θ diffraction measurements. The strain of the films was careful studied by performing reciprocal space maps around some selected LMO Bragg peaks. The relative concentration of La and Mn cations in the deposited films was studied by Wavelength Dispersive Spectrometer (WDS) microprobe analysis. X-ray absorption spectroscopy (XAS) at the Mn $L_{2/3}$ edge was measured at BESSY II in total electron yield (TEY) configuration. Magnetic properties were measured in a commercial SQUID magnetometer (Quantum Design). Field-cooled temperature dependent magnetization measurements and magnetic hysteresis loops were performed up to applied magnetic fields of 70 kOe between 10K and 250 K. Magnetic field was applied parallel to the substrate plane. The diamagnetic contribution of the STO substrate was accurately subtracted by measuring magnetization loops at 300K and assuming a temperature independent susceptibility.

RESULTS AND DISCUSSION

Magnetic and transport properties of LMO thin films as a function of $PO_2$ during the growth process are shown in Figure 1. The evolution of the temperature dependent magnetization (measured at 5 kOe) is plotted in Fig 1(a) while M(H) curves at 5K are plotted in Fig. 1 (b). It is evident from the figures that films grown at the lowest available pressure ($PO_2 \sim 5x10^{-3}$ mTorr) show a negligible magnetization from 300K down to 140 K. At this temperature there is a slight cusp in the M(T) curve and, then, magnetization increases up to a value of 0.25 $\mu_B$/f.u. This dependence is consistent with the canted AF behavior usually reported for bulk stoichiometric LMO material with $T_N$~140K and a residual moment of 0.16 $\mu_B$/f.u. at 10K.[24] In our case, M(T) dependence below 100K suggest the existence of a antiferromagnet where some uncompensated

moments are responsible for the slightly higher residual magnetization. Hysteresis loops also reflect the change of magnetic properties for the different samples. It is evident from Fig. 1(b) that coercivity diminishes as magnetization increases. Moreover, M(H) loops for samples grown below $PO_2$ =0.1 mTorr could correspond to an AF material in a background of unbalanced magnetic moments. As $PO_2$ is increased during deposition the magnetization of films progressively rises. At the highest available $PO_2$, i.e., $PO_2$ ~ 200 mTorr, LMO films show a robust ferromagnetic behavior with $T_C$ ~200 K and $M_s$(10K) ~ 3.6 $\mu_B$/f.u (as determined from MvsH curves). This result is to be compared either with 4 $\mu_B$/f.u. expected for $Mn^{3+}$ ions or with a 40% content of $Mn^{4+}$ in a double exchange scenario. Possible variations on the Mn oxidation state between different samples have been evaluated by means of XAS experiments. It has been previously reported that as Mn valence is increased, Mn $L_3$ edge peak shifts towards higher energies (almost 1.5-2 eV in the case of $Mn^{3+}$to $Mn^{4+}$) and the ratio of $L_3$ (~642.5 eV) to $L_2$ (~653.5 eV) intensity decreases[25-26]. Figure 1(c) shows the TEY spectra around the $L_{2/3}$ edge for three different films prepared under different $PO_2$ partial pressures. Neither energy shift in the peak position nor overall change of the spectral shape on the $PO_2$ partial pressures can be detected. This result clearly indicates that the $Mn^{3+}/Mn^{4+}$ ratio remains unchanged through the whole series of samples. The small shoulder observed around 640eV in the sample grown at 200mTorr may be attributed to the presence of $Mn^{2+}$ formed at the surface of the film after exposure to air as previously reported for manganite films.[27] Temperature dependence of the electrical resistivity of the LMO thin films is depicted in Fig. 1 (d). All the measured samples exhibit insulating behavior with no sign of metallic-insulating transition within our accessible range of resistances. The electronic transport properties of LMO films may be affected by the presence of La/Mn vacancies. It is usually observed that La vacancies promote metallic behavior

by a double exchange mechanism while doping induced by Mn vacancies is claimed to lead to insulating behavior.[10-11, 13-14] To exclude this scenario it is crucial to ensure a stoichiometric 1:1 La:Mn relationship in all the films. WDS results, shown in the Inset of Figure 1(c), indicate that this is the case, except for a small La deficiency detected in samples grown at the lowest $PO_2$. For these samples grown at the lowest $PO_2$ WDS results indicate a La:Mn ratio of about 0.97. Thus, suggesting that the generation of La vacancies is the mechanism to accommodate oxygen vacancies during the growth process in reducing atmosphere. Therefore, for samples grown at the lowest $PO_2$, assuming no change in the Mn oxidation state, charge equilibrium would lead to a film composition of $La_{0.97}MnO_{3+\delta}$, clearly in the AF-I region of the phase diagram. In all the other samples, even at high oxygen pressures, La:Mn ratio is 1 and the above arguments cannot be invoked to explain the observed transport properties.

As mentioned in the introduction, the electronic properties of LMO samples may also be affected by structural strain. In this regard, it is worth mentioning that epitaxial accommodation of the highly distorted orthorhombic LMO structure onto cubic STO substrates is not trivial. We recall that at thin film growth temperatures (T= 850ºC), stoichiometric bulk LMO crystallizes in a Pbnm orthorhombic structure with pseudocubic parameters $a/\sqrt{2} \sim b/\sqrt{2} \sim c/2 \sim 0.3932$ nm.[28] At 750K, a cooperative Jahn-Teller transition takes place and even the structure is still described by a orthorhombic Pbnm space group, $MnO_6$ octahedra are highly distorted and cell parameters change to a = 0.5533nm, b = 0.5727 nm, c = 0.7668nm (at 300K).[6] As a result, two different Mn-Mn matching distances are found, 0.3982 nm in the ab-plane and 0.3834 nm along c-axis, resulting in about -2% compressive or +2% tensile mismatching, respectively. In oxygen rich atmosphere, La and/or Mn vacancies may be created to accommodate oxygen off-stoichiometry although, for clarity, $LaMnO_{3+\delta}$ notation is commonly used in the literature. Pbnm symmetry is

maintained and lattice parameters vary then as a function of this oxygen excess up to values of a = 0.5507 nm, b = 0.5495 nm, c = 0.7766 nm for $\delta$= 0.07 [7]. In this case, Mn-Mn distances are 0.3890 nm in-plane and 0.3883 nm out-of-plane. Here, strain induced by STO substrate ($a_{STO}$=0.3905nm) is tensile both in parallel and perpendicular configuration and lower than 0.6%. At higher values of $\delta$, the phase is no longer described by Pbnm space group and instead a rhombohedral R3c structure is found.[5-7] Due to the close competing epitaxial relationships, it is important to first determine if LMO growths with its c-axis parallel or perpendicular to the plane of the substrate as schematically indicated in Figure 2(a) and (b). To distinguish between these two possible crystallographic orientations we have performed a series of phi-scans around integer and half-integer reflections. These half-Integer Bragg peaks are associated to the rotations of oxygen octahedral and their occurrence (or absence) is used to determine the orientation of LMO orthorhombic c-axis relative to substrate. [29-30] In particular, assuming h, k, l Miller indexes following the reciprocal space axes $Q_x$, $Q_y$ and $Q_z$, of a primitive cubic cell, when c-axis is contained in the plane of the substrate reflections of the type h/2,k,l (with h=odd) appear while h,k,l/2 with l=odd are only present if LMO c-axis is out-of-plane. Reflections of the type (h/2,k/2,l/2) with all index h,k,l being odd are allowed for both orientations. In figures 2(c) and (d) we have plotted a two dimensional projection of the reciprocal space map (in units of STO cell) with $Q_{ip}=\sqrt{(Q_x^2+Q_y^2)}$ being the in-plane component (referred to substrate) and $Q_z$ component of momentum perpendicular to substrate. For both samples, reflections with integer h,k,l are masked by those of the STO substrate while reflections of the type (h/2,k,l) are observed and those of the type (h,k,l/2) are absent. This result is consistent with orthorhombic LMO with c-axis in-plane following both [100] and [010] directions of the STO substrate (Figure 2(a)). Note that this epitaxial relationship has important implications on the analysis of the expected

magnetic behaviour of the films as ab-planes are lying perpendicular to the substrate and the expected staggered orbital ordering leading to the AF state will be out-of-plane arranged as schematically shown in Fig. 2 (a).

As LMO thin films reflections are difficult to resolve from those of substrate, resolution of usual reciprocal space maps (for example, using 114 reflection) are not enough to elucidate the in-plane strain state of the LMO thin films. For this, we have performed high-resolution reciprocal space maps around hk0 reflections with grazing incidence. In this experimental configuration, low x-ray penetration minimizes the substrate signal and information on LMO thin film can be accurately obtained. Figures 3(a) and (b) show reciprocal space maps around 200 reflections for the same samples as in Figure 2. We see (Fig. 3 (a)) that the sample grown under low $PO_2$ presents a microstructure with well defined twinned domains corresponding to two different in-plane cell parameters of 0.3946 nm and 0.3866 nm. Comparing with the expected bulk values (0.3982nm and 0.3834 nm) we may conclude that film is partially relaxed. The cross shape of the in-plane map is consistent with the formation of (110) twin planes inducing a slight in-plane rotation of the domains, which produces the spread in $\phi$ angle shown in the map. On the contrary, for films grown under oxidizing atmospheres, only one clear peak is observed and in-plane parameters match those of the underlying substrate $a_{STO}$=0.3905 nm (Fig. 3 (b)). In this case, LMO films are fully strained. Films grown at intermediate oxygen pressures exhibit different degrees of strain. A way to monitor this continuous evolution of the microstructural strain state of the films has been possible by studying the equivalent out-of-plane pseudocubic lattice parameter. The out-of-plane values obtained by fitting the $\theta$-$2\theta$ (002 LMO + 002 STO) high resolution XRD profiles are plotted in Figure 4(a) as a function of oxygen partial pressure during deposition. Error bars, determined from the standard deviation of the least

squares fit increase as LMO peak position approaches that of the underlying substrate. We may observe that out-of-plane parameter ranges from values as high as 0.400 nm when LMO is grown under reducing conditions down to 0.392 nm, i.e., close to the STO lattice parameter in highest $pO_2$ atmosphere. This structural evolution is concomitant to the variation of the functional properties presented above and, indeed, there is a close relationship between saturation magnetization and out-of-plane parameter as shown in Figure 4 (b). In light of these findings a plausible scenario emerges to account for spread of experimental results reported on LMO thin films. At reducing atmospheres, LMO thin films are partially relaxed, with their structure close to that of stoichiometric bulk compound. Cooperative Jahn-Teller distortions lead to the stabilization of a staggered $d_{3x^2-r^2}/d_{3y^2-r^2}$ ordering resulting in an A-type AF-I state. However, magnetic moments are supposed to be aligned along the orthorhombic b axis that, in twinned films, is pointing out of the substrate at four possible directions forming 45º with the direction perpendicular to the film substrate. As a consequence, it is difficult to observe a clean and net AF response. This twinned structure, leading to antiferromagnetic domain walls could account also for the residual magnetic moment observed in the AF phase. In films deposited at progressively higher $pO_2$, film substrate mismatch is reduced, allowing a coherent epitaxial growth of fully strained films. In this situation, strain modifies the usual Jahn-Teller distortion picture and different orbital orderings are possible. In our case, a FM-I phase is stabilized compatible with recent theoretical proposals suggesting a three-dimensional $d_{3z^2-r^2}/$ $d_{x^2-y^2}$orbital ordering [23]. Note that, in both cases, the expected orbital arrangements lead to a mixing of occupied out-of-plane and in-plane orbitals (see Figure 2). Thus, the usual synchrotron techniques to study orbital occupancy as, for example, x-ray linear dichroism (XLD) are not longer straightforward to apply. Furthermore, the presence of twinned microstructures would

make almost impossible to derive any solid conclusion about selective orbital occupancy from XLD measurements. Nevertheless, our results showed that studying the possible orbital and magnetic arrangements and the role of cooperative Jahn-Teller distortions in the parent compound $LaMnO_3$ and other reported FMI phases as, for example, low doped $La_{1-x}Sr_xMnO_3$ deserves further attention[31-32].

## CONCLUSIONS

In summary, we have carefully studied the epitaxial growth process of $LaMnO_3$ thin films on STO substrates demonstrating that the accommodation of the LMO orthorhombic structure onto STO cubic structure is a complex process that can be properly controlled by modifying the nominal oxygen pressure during growth process. This structural accommodation imply a substantial modification of the amount of structural strain in the LMO film that, in turns, have subtle effects on the final magnetic and electronic properties of the films. Our results show that films with bulk-like AF-I properties are obtained only when growing under reducing atmospheres that lead to partially relaxed structures. In contrast, when film growth takes place under oxidizing conditions, fully strained films exhibiting a FM-I behavior are obtained. Other scenarios, such as La or Mn vacancies, leading to a variation of the Mn oxidation state have been excluded in base of WDS and XAS measurements. Although further spectroscopic research may be necessary to get a complete picture of the magnetic and orbital arrangements while still disregarding doping effects, our results strongly point to a strain-induced selective orbital occupancy as the origin of the observed FM behaviour in agreement with recent theoretical calculations.

FIGURES

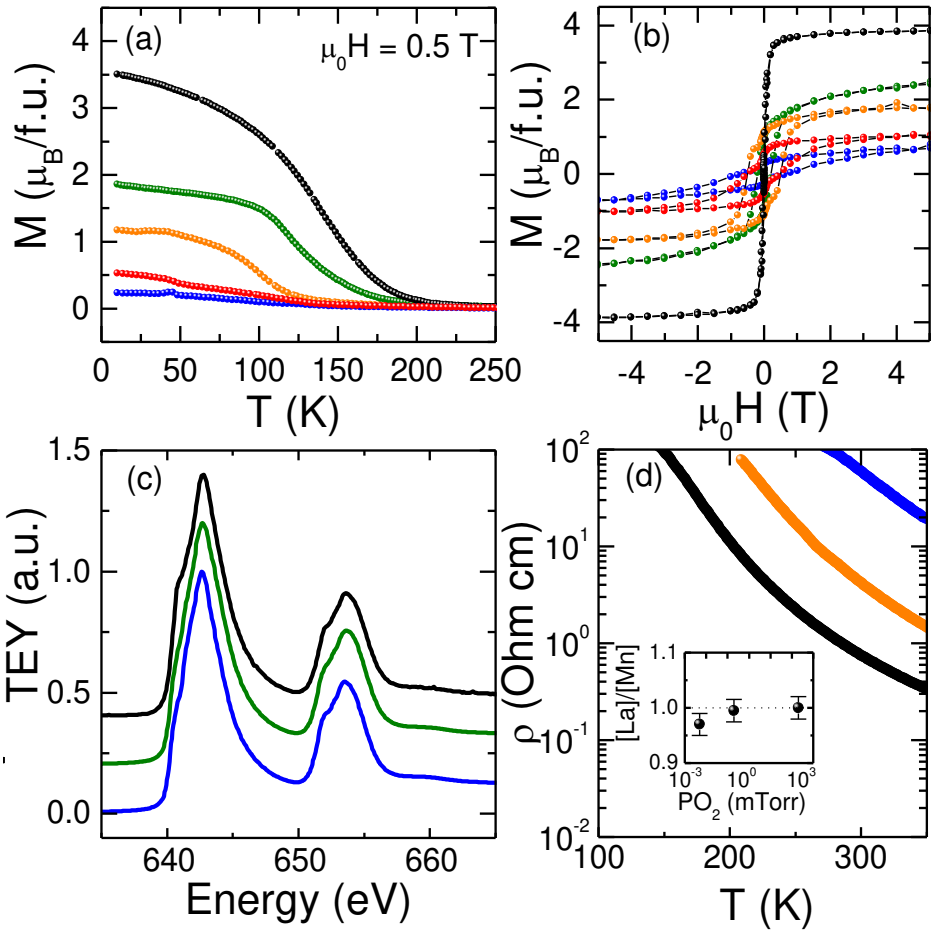


**Figure 1.** Magnetic and electronic properties of LMO thin films grown at different oxygen pressures, $PO_2$= 200mTorr (black), 40mTorr (green), 0.2mTorr (orange), 0.04mTorr (red) and $5x10^{-3}$ mTorr(blue). (a) Temperature dependence of magnetization measured at 0.5T. (b) Hysteresis loops at 10K. Diamagnetic contribution of substrate has been removed. (c) Manganese L-edge XAS spectra measured by TEY for three different LMO samples showing that no significant change in the $Mn^{3+}/Mn^{4+}$ ratio is observed. (d) Temperature dependence of the electrical resistivity. Inset of (d) shows the La:Mn ratio as measured from WDS.

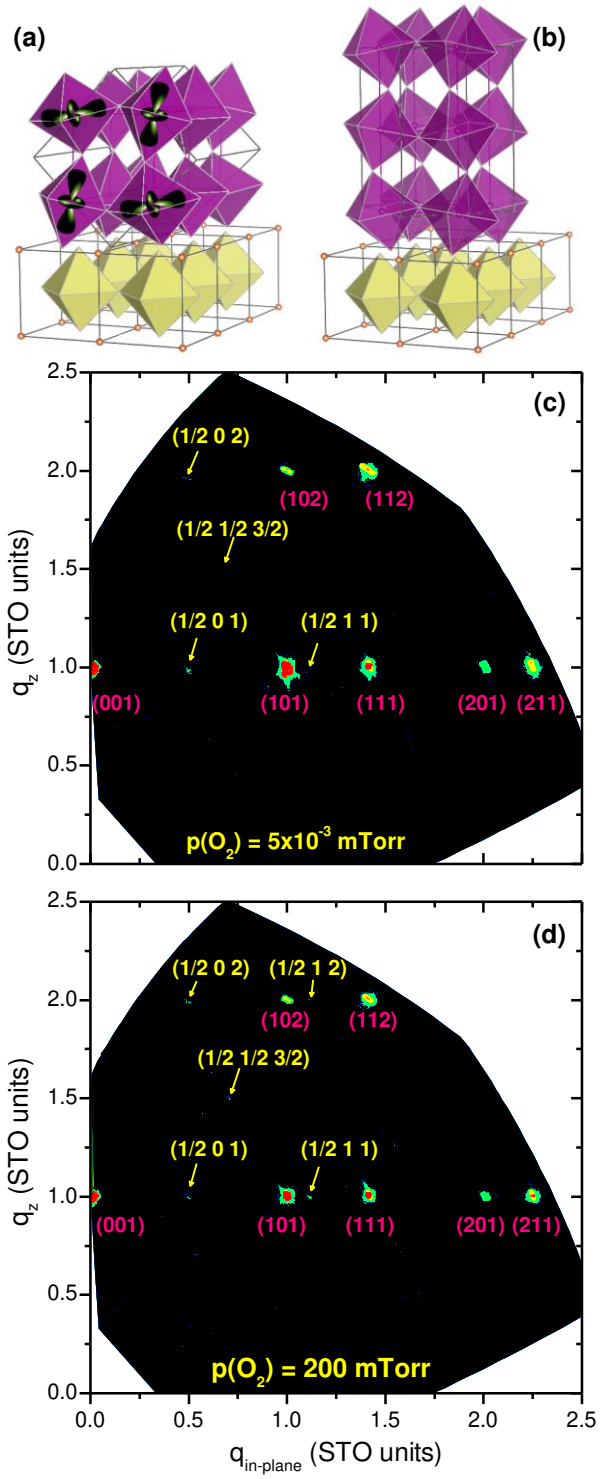


**Figure 2.** Schematic representation of the possible crystallographic orientation of LMO thin films, either with orthorhombic c-axis in the plane of the substrate (a) or perpendicular to it (b).

Schema of the expected orbital ordering leading to antiferromagnetic state is shown in (a). (c) and (d) are two dimensional projections of the reciprocal space map for the samples grown at the lowest ($5x10^{-3}$ mTorr) and highest (200mTorr) oxygen pressures respectively. For clarity, STO substrate units are used by taking $a_{STO}$=0.3905 nm. Reflections are labeled in yellow showing that only half-integer reflections of the kind (h/2,k,l) are observed, compatible with crystallographic orientation in (a). Integer LMO reflections are masked by those of the STO substr ate (labeled in violet).

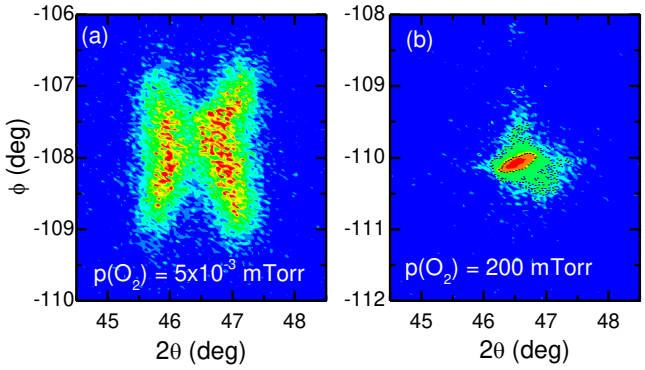


**Figure 3** In-plane reciprocal space maps around 200 reflections of samples grown at (a) the lowest ($5x10^{-3}$ mTorr) and (b) highest (200mTorr) oxygen pressures.

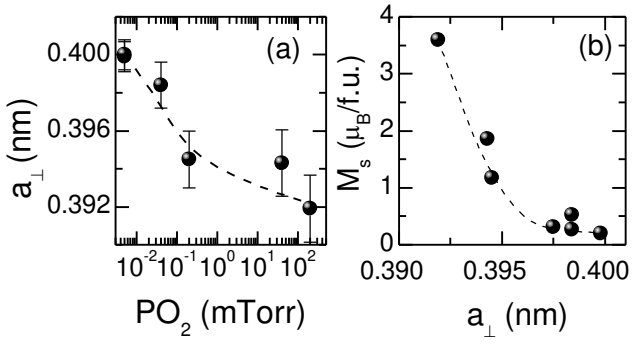


**Figure 4** (a) Variation of the out-of-plane lattice parameter (referred to pseudocubic lattice) of LMO thin films as a function of oxygen pressure. (b) Dependence of saturation magnetization with out-of-plane lattice parameter.

AUTHOR INFORMATION

**Corresponding Author**

*E-mail: apomar@icmab.es. Tel: + 34-93-580-18-53. Fax: +34-93-580-57-29

ACKNOWLEDGMENT

We acknowledge financial support from the Spanish MINECO (MAT2011-29081 and MAT2012-33207), CONSOLIDER (CSD2007-00041), and FEDER program. We thank P. García for his kind assistance during x-ray experiments. ICN2 acknowledges support from the Severo Ochoa Program (MINECO, Grant - SEV 2013-0295). ZK thanks the support from the Ministry of Education, Science, and Technological Development of Republic of Serbia through Project III45018.

REFERENCES

1. Gibert, M.; Zubko, P.; Scherwitzl, R.; Iniguez, J.; Triscone, J. M., Exchange bias in $LaNiO_3$-$LaMnO_3$ superlattices. *Nat Mater* **2012,** *11*, 195-198

2. Garcia-Barriocanal, J.; Bruno, F. Y.; Rivera-Calzada, A.; Sefrioui, Z.; Nemes, N. M.; Garcia-Hernandez, M.; Rubio-Zuazo, J.; Castro, G. R.; Varela, M.; Pennycook, S. J.; Leon, C.; Santamaria, J., "Charge Leakage" at $LaMnO_3$/$SrTiO_3$ Interfaces. *Adv Mater* **2010,** *22*, 627-+

3. Garcia-Barriocanal, J.; Cezar, J. C.; Bruno, F. Y.; Thakur, P.; Brookes, N. B.; Utfeld, C.; Rivera-Calzada, A.; Giblin, S. R.; Taylor, J. W.; Duffy, J. A.; Dugdale, S. B.; Nakamura, T.; Kodama, K.; Leon, C.; Okamoto, S.; Santamaria, J., Spin and orbital Ti magnetism at $LaMnO_3$/$SrTiO_3$ interfaces. *Nat Commun* **2010,** *1*, 82

4. Bhattacharya, A.; May, S. J.; Velthuis, S. G. E. T.; Warusawithana, M.; Zhai, X.; Jiang, B.; Zuo, J. M.; Fitzsimmons, M. R.; Bader, S. D.; Eckstein, J. N., Metal-insulator transition and its relation to magnetic structure in $(LaMnO_3)_{2n}$/$(SrMnO_3)_n$ superlattices. *Phys Rev Lett* **2008,** *100*, 257203

5. Topfer, J.; Goodenough, J. B., $LaMnO_{3+delta}$ revisited. *J Solid State Chem* **1997,** *130*, 117-128

6. Huang, Q.; Santoro, A.; Lynn, J. W.; Erwin, R. W.; Borchers, J. A.; Peng, J. L.; Greene, R. L., Structure and magnetic order in undoped lanthanum manganite. *Phys. Rev. B* **1997,** *55*, 14987-14999

7. Ritter, C.; Ibarra, M. R.; DeTeresa, J. M.; Algarabel, P. A.; Marquina, C.; Blasco, J.; Garcia, J.; Oseroff, S.; Cheong, S. W., Influence of oxygen content on the structural, magnetotransport, and magnetic properties of $LaMnO_{3+delta}$. *Phys. Rev. B* **1997,** *56*, 8902-8911

8. Aruta, C.; Angeloni, M.; Balestrino, G.; Boggio, N. G.; Medaglia, P. G.; Tebano, A.; Davidson, B.; Baldini, M.; Di Castro, D.; Postorino, P.; Dore, P.; Sidorenko, A.; Allodi, G.; De Renzi, R., Preparation and characterization of $LaMnO_3$ thin films grown by pulsed laser deposition. *J Appl Phys* **2006,** *100*, 023910

9. Orgiani, P.; Aruta, C.; Ciancio, R.; Galdi, A.; Maritato, L., Enhanced transport properties in $La_xMnO_{3-delta}$ thin films epitaxially grown on $SrTiO_3$ substrates: The profound impact of the oxygen content. *Appl Phys Lett* **2009,** *95*, 013510

10. Kim, H. S.; Christen, H. M., Controlling the magnetic properties of $LaMnO_3$ thin films on $SrTiO_3$(100) by deposition in a $O_2$/Ar gas mixture. *J Phys-Condens Mat* **2010,** *22*, 146007

11. Choi, W. S.; Marton, Z.; Jang, S. Y.; Moon, S. J.; Jeon, B. C.; Shin, J. H.; Seo, S. S. A.; Noh, T. W.; Myung-Whun, K.; Lee, H. N.; Lee, Y. S., Effects of oxygen-reducing atmosphere annealing on $LaMnO_3$ epitaxial thin films. *J Phys D Appl Phys* **2009,** *42*, 165401

12. Marton, Z.; Seo, S. S. A.; Egami, T.; Lee, H. N., Growth control of stoichiometry in $LaMnO_3$ epitaxial thin films by pulsed laser deposition. *J Cryst Growth* **2010,** *312*, 2923-2927

13. Choi, W. S.; Jeong, D. W.; Jang, S. Y.; Marton, Z.; Seo, S. S. A.; Lee, H. N.; Lee, Y. S., $LaMnO_3$ Thin Films Grown by Using Pulsed Laser Deposition and Their Simple Recovery to a Stoichiometric Phase by Annealing. *J Korean Phys Soc* **2011,** *58*, 569-574

14. Marozau, I.; Das, P. T.; Dobeli, M.; Storey, J. G.; Uribe-Laverde, M. A.; Das, S.; Wang, C. N.; Rossle, M.; Bernhard, C., Influence of La and Mn vacancies on the electronic and magnetic properties of $LaMnO_3$ thin films grown by pulsed laser deposition. *Phys. Rev. B* **2014,** *89*, 174422

15. Orgiani, P.; Galdi, A.; Aruta, C.; Cataudella, V.; De Filippis, G.; Perroni, C. A.; Ramaglia, V. M.; Ciancio, R.; Brookes, N. B.; Moretti Sala, M.; Ghiringhelli, G.; Maritato, L.,

Multiple double-exchange mechanism by $Mn^{2+}$ doping in manganite compounds. *Phys. Rev. B* **2010,** *82*, 205122

16. Galdi, A.; Aruta, C.; Orgiani, P.; Brookes, N. B.; Ghiringhelli, G.; Moretti Sala, M.; Mangalam, R. V. K.; Prellier, W.; Luders, U.; Maritato, L., Magnetic properties and orbital anisotropy driven by $Mn^{2+}$ in nonstoichiometric $La_xMnO_{3-delta}$ thin films. *Phys. Rev. B* **2011,** *83*, 064418

17. Ahn, K. H.; Millis, A. J., Effects of in-plane strain on magnetism in $LaMnO_3$ thin films. *Int J Mod Phys B* **2002,** *16*, 3281-3284

18. Nanda, B. R. K.; Satpathy, S., Effects of strain on orbital ordering and magnetism at perovskite oxide interfaces: LaMnO(3)/SrMnO(3). *Phys. Rev. B* **2008,** *78*, 054427

19. Nanda, B. R. K.; Satpathy, S., Magnetic and orbital order in $LaMnO_3$ under uniaxial strain: A model study. *Phys. Rev. B* **2010,** *81*, 064418

20. Nanda, B. R. K.; Satpathy, S., Density functional studies of $LaMnO_3$ under uniaxial strain. *J Magn Magn Mater* **2010,** *322*, 3653-3657

21. Lee, J. H.; Delaney, K. T.; Bousquet, E.; Spaldin, N. A.; Rabe, K. M., Strong coupling of Jahn-Teller distortion to oxygen-octahedron rotation and functional properties in epitaxially strained orthorhombic $LaMnO_3$. *Phys. Rev. B* **2013,** *88*, 174426

22. Solovyev, I.; Hamada, N.; Terakura, K., Crucial role of the lattice distortion in the magnetism of $LaMnO_3$. *Phys Rev Lett* **1996,** *76*, 4825-4828

23. Hou, Y. S.; Xiang, H. J.; Gong, X. G., Intrinsic insulating ferromagnetism in manganese oxide thin films. *Phys. Rev. B* **2014,** *89*, 064415

24. Skumryev, V.; Ott, F.; Coey, J. M. D.; Anane, A.; Renard, J. P.; Pinsard-Gaudart, L.; Revcolevschi, A., Weak ferromagnetism in $LaMnO_3$. *Eur Phys J B* **1999,** *11*, 401-406

25. Cramer, S. P.; Degroot, F. M. F.; Ma, Y.; Chen, C. T.; Sette, F.; Kipke, C. A.; Eichhorn, D. M.; Chan, M. K.; Armstrong, W. H.; Libby, E.; Christou, G.; Brooker, S.; McKee, V.; Mullins, O. C.; Fuggle, J. C., Ligand-field strengths and oxidation states from manganese L-edge spectroscopy. *J. Am. Chem. Soc.* **1991,** *113*, 7937-7940

26. Qiao, R. M.; Chin, T.; Harris, S. J.; Yan, S. S.; Yang, W. L., Spectroscopic fingerprints of valence and spin states in manganese oxides and fluorides. *Curr. Appl. Phys.* **2013,** *13*, 544-548

27. Valencia, S.; Gaupp, A.; Gudat, W.; Abad, L.; Balcells, L.; Cavallaro, A.; Martinez, B.; Palomares, F. J., Mn valence instability in $La_{2/3}Ca_{1/3}MnO_3$ thin films. *Phys. Rev. B* **2006,** *73*, 7104402

28. Chatterji, T.; Fauth, F.; Ouladdiaf, B.; Mandal, P.; Ghosh, B., Volume collapse in $LaMnO_3$ caused by an orbital order-disorder transition. *Phys. Rev. B* **2003,** *68*, 052406

29. Johnson-Wilke, R. L.; Marincel, D.; Zhu, S.; Warusawithana, M. P.; Hatt, A.; Sayre, J.; Delaney, K. T.; Engel-Herbert, R.; Schlepütz, C. M.; Kim, J. W.; Gopalan, V.; Spaldin, N. A.; Schlom, D. G.; Ryan, P. J.; Trolier-McKinstry, S., Quantification of octahedral rotations in strained $LaAlO_3$ films via synchrotron x-ray diffraction. *Phys. Rev. B* **2013,** *88*, 174101

30. May, S. J.; Kim, J. W.; Rondinelli, J. M.; Karapetrova, E.; Spaldin, N. A.; Bhattacharya, A.; Ryan, P. J., Quantifying octahedral rotations in strained perovskite oxide films. *Phys. Rev. B* **2010,** *82*, 014110

31. Geck, J.; Wochner, P.; Kiele, S.; Klingeler, R.; Reutler, P.; Revcolevschi, A.; Büchner, B., Orbital Polaron Lattice Formation in Lightly Doped $La_{1-x}Sr_xMnO_3$. *Phys Rev Lett* **2005,** *95*, 236401

32. Golenishchev-Kutuzov, A. V.; Golenishchev-Kutuzov, V. A.; Kalimullin, R. I.; Semennikov, A. V., Ordered states of Jahn-Teller distorted $MnO_6$ octahedra in weakly doped lanthanum-strontium manganites. *Phys. Solid State* **2015,** *57*, 1633-1638

**Table of Contents Graphic**

The amount of structural strain in Pulsed Laser Deposited $LaMnO_3$ thin films is controlled by modifying the nominal oxygen pressure during growth. Bulk-like antiferromagnetic films are obtained when reducing conditions lead to partially relaxed films. On the opposite under oxidizing conditions, fully strained films exhibit ferromagnetic insulating behavior related to strain-induced orbital ordering.